RESEARCH PAPER

Nucleus 1:3, 273-283; May/June 2010 © 2010 Landes Bioscience

Dynamic properties of meiosis-specific lamin C2 and its impact on nuclear envelope integrity

Daniel Jahn, Sabine Schramm, Ricardo Benavente and Manfred Alsheimer*

Department of Cell and Developmental Biology; Biocenter; University of Würzburg; Würzburg, Germany

Key words: germ cells, spermatogenesis, meiosis, spermatocytes, nuclear envelope, nuclear lamina, lamin C2, A-type lamins

Abbreviations: INM, inner nuclear membrane; IF, intermediate filament; NPC, nuclear pore complex; NE, nuclear envelope; NLS, nuclear localization signal; EGFP, enhanced green fluorescent protein; FRAP, fluorescence recovery after photobleaching; FLIP, fluorescence loss in photobleaching; MEF, murine embryonic fibroblast; myr, recognition motif for N-myristoylation; ROI, region of interest; mAb, monoclonal antibody; pAb, polyclonal antibody

A hallmark of meiosis is the precise pairing and the stable physical connection (synapsis) of the homologous chromosomes. These processes are essential prerequisite for their proper segregation. Pairing of the homologs during meiotic prophase I critically depends on characteristic movements of chromosomes. These movements, in turn, require attachment of meiotic telomeres to the nuclear envelope and their subsequent dynamic repositioning. Dynamic repositioning of meiotic telomeres goes along with profound structural reorganization of the nuclear envelope. The short A-type lamin C2 is thought to play a critical role in this process due to its specific expression during meiotic prophase I and the unique localization surrounding telomere attachments. Consistent with this notion, here we provide compelling evidence that meiosis-specific lamin C2 features a significantly increased mobility compared to somatic lamins as revealed by photobleaching techniques. We show that this property can be clearly ascribed to the lack of the N-terminal head and the significantly shorter α-helical coil domain. Moreover, expression of lamin C2 in somatic cells induces nuclear deformations and alters the distribution of the endogenous nuclear envelope proteins lamin B1, LAP2, SUN1 and SUN2. Together, our data define lamin C2 as a "natural lamin deletion mutant" that confers unique properties to the nuclear envelope which would be essential for dynamic telomere repositioning during meiotic prophase I.

Introduction

The nuclear lamina is a polymeric protein meshwork intimately associated with the nucleoplasmic surface of the inner nuclear membrane (INM). Its major components are the nuclear lamins which belong to the family of intermediate filament (IF) proteins and are the only known members of this family localized in the nucleus.[1,2] Lamins interact both with integral membrane proteins of the INM and with chromatin. Besides providing mechanical stability to the nucleus, the nuclear lamina is involved in several fundamental cellular processes such as chromatin organization, gene expression and anchoring of nuclear pore complexes (NPCs), thus fulfilling critical functions for cell viability.[3-5] As supported by a large body of evidence, dysfunctions concerning the nuclear lamina give rise to severe human disorders collectively termed laminopathies.[6,7]

Nuclear lamins are subdivided in A-type and B-type lamins. These differ with regard to their biochemical properties, their behavior during mitotic nuclear envelope (NE) disassembly and their expression pattern in ontogenesis.[8-10] B-type lamins present in mammalian somatic cells, namely lamins B1 and B2, are encoded by two different genes (*Lmnb1* and *Lmnb2*).[11,12] B-type lamins are essential for cell viability and at least one of them is expressed throughout development.[13] A-type lamins of mammalian somatic cells, namely lamins A and C, are alternative splice variants arising from one single gene (*Lmna*) and their expression is differentially regulated in a development-dependent, tissue-specific manner.[14,15]

Lamins display a typical tripartite structure common for all IF proteins comprising an N-terminal globular head domain, a central α-helical rod domain and a C-terminal non-helical tail, which for nuclear lamins adopts an immunoglobulin-like fold (Ig-fold). A couple of mutations in the human *LMNA* gene leading to different forms of muscular dystrophy and lipodystrophy were reported to cluster in the region encoding the Ig-fold of lamins A/C.[16,17] Several studies analyzing IF assembly demonstrated that the α-helical rod together with the globular head promote IF protein dimerization and the formation of higher-order polymers.[10,18,19] Recruitment of lamins B1, B2 and A to the INM relies on the presence of a nuclear localization signal (NLS) within the lamin tail and a C-terminal CaaX motif which is target for several post-translational modifications including farnesylation, proteolytic trimming and carboxy-methylation.[20-24] B-type lamins remain permanently farnesylated, whereas the farnesylated

*Correspondence to: Manfred Alsheimer; Email: alsheimer@biozentrum.uni-wuerzburg.de
Submitted: 02/05/10; Revised: 03/12/10; Accepted: 03/15/10
Previously published online: www.landesbioscience.com/journals/nucleus/article/11800

C-terminus of lamin A is removed by proteolytic cleavage soon after its incorporation into the nuclear lamina.[25] Lamin C is exceptional as it lacks a CaaX motif and its recruitment to the nuclear lamina therefore depends on other lamins.[26-28]

Compared to somatic cells, the nuclear lamina composition of mammalian spermatogenic cells is remarkably different. While lamins B2, A and C are absent during the entire process of spermatogenesis, lamin B1 is the only somatic lamin variant detectable in these cells.[29] However, spermatogenic cells express two germ line-specific lamin variants, namely lamins C2 and B3, which are alternatively spliced isoforms arising from the *Lmna* and the *Lmnb2* gene, respectively.[30,31] Whereas lamin C2 is exclusively expressed during meiotic stages of spermatogenesis, the expression of lamin B3 is restricted to post-meiotic stages (i.e., spermiogenesis).[32-35] An important common structural feature of both spermatogenesis-specific lamins is their N-terminal truncation resulting in the complete lack of the N-terminal head domain and a significant portion of the α-helical rod domain.[31,33,34] These lacking domains are replaced by unique N-terminal amino acid sequences. In the case of lamin C2, this is the hexapeptide GNAEGR, which serves as a recognition motif for N-myristoylation essential for NE targeting of lamin C2.[36] As the domains lacking in both lamin C2 and B3 were shown to be important for lamin assembly,[10,18,19] it has repeatedly been proposed that these shortened, spermatogenesis-specific lamins could modulate the structural integrity of the nuclear lamina in spermatogenic cells thus facilitating spermatogenesis-specific events.[31,32,34,37]

The remarkable alterations concerning nuclear lamina composition of spermatogenic cells correlate with profound changes in the nuclear interior. Early in meiotic prophase I telomeres of meiotic chromosomes become attached to the NE and subsequently cluster in a spatially distinct area. Dynamic telomere repositioning results in the formation of the chromosomal bouquet at leptotene/zygotene transition which is an evolutionarily conserved and most central feature of meiotic prophase I. Dynamic telomere repositioning continues throughout mid-prophase I leading to the resolution of the bouquet configuration and ongoing oscillatory chromosome movements during pachytene. Together, these processes are thought to play a vital role for proper pairing and synapsis of the homologous chromosomes.[38-41] Several observations point to a specific function of meiosis-specific lamin C2 for the attachment and/or the dynamic repositioning of meiotic telomeres. First, the expression of lamin C2 is restricted to meiotic prophase I and therefore temporally correlates with these events.[32-34] Second, contrary to somatic lamins, meiosis-specific lamin C2 is not distributed in a continuous rim-like pattern at the NE but rather is enriched in discontinuous domains. Interestingly, in mammalian spermatocytes NE-attached telomeres of meiotic chromosomes were found to localize solely within these lamin C2-containing domains.[37] With regard to this temporal and spatial expression as well as its structural peculiarities described above, it was hypothesized that meiosis-specific lamin C2 could modulate the structural integrity of the nuclear lamina at the sites of telomere attachment, thus allowing for the attachment and/or dynamic repositioning of telomeres during meiotic prophase I. However, whether the discrete lamin C2-containing domains represent local reinforcements or rather constitute dynamic platforms for telomere movement has not been clarified so far.

To address this issue, in the present study we performed a detailed analysis of the dynamic properties of meiosis-specific lamin C2. Our results provide clear evidence that lamin C2 features a significantly increased mobility compared to its somatic counterpart lamin C. We found that the lack of either the N-terminal head or the N-terminal part of the α-helical rod domain alone was sufficient to establish this increased mobility. Furthermore, we show that ectopic expression of lamin C2 in somatic cells induces nuclear deformations and alters the distribution of endogenous NE proteins. Together, our data provides novel insights into the physiological properties of meiosis-specific lamin C2 that improve our understanding of the molecular mechanism underlying the distinct function of lamin C2 for dynamic telomere repositioning during meiotic prophase I.

Results

Meiosis-specific lamin C2 features an increased mobility compared to its somatic counterpart lamin C. Meiosis-specific lamin C2 is an N-terminally truncated splice variant of the *Lmna* gene lacking domains that are known to be important for lamin assembly. For this reason, we assumed that lamin C2 has the competence to modify the structural integrity of the NE. To address this issue on the molecular level we analyzed the dynamic properties of lamin C2-EGFP fusion proteins by FRAP and FLIP experiments (overview of constructs in **Fig. 1A**). In contrast to differentiated somatic cells, lamins A/C are absent in the natural meiotic environment of lamin C2 (i.e., spermatocytes).[29] Since meiotic cells themselves are not well suited for in vitro manipulation we mimicked this condition in our experimental system and performed all photobleaching experiments in *Lmna*$^{-/-}$ MEFs which do not express endogenous lamins A/C.[42] As a control we used lamin C which is the somatic counterpart of lamin C2. Contrary to other somatic lamins, wild type lamin C lacks an endogenous NE targeting motif.[43] Consequently, its overexpression results in the formation of nucleoplasmic aggregates.[36] In order to direct lamin C to the NE we fused the myristoylation motif of lamin C2 (i.e., GNAEGR; in the following referred to as "myr") to the N-terminus of lamin C thus generating a protein construct (myr-lamin C-EGFP) with an identical mechanism of NE targeting compared to lamin C2. Therefore, possible differences in the dynamic properties of the analyzed proteins caused by different mechanisms of NE recruitment could be excluded a priori.

In our photobleaching experiments myr-lamin C-EGFP localized at the NE in a rim-like pattern typical for somatic lamin variants. In contrast, lamin C2-EGFP localized at the NE of transfected somatic cells in discontinuous domains in the following referred to as discrete "plaques" (**Fig. 1C**). This observation is consistent with previous studies.[36] In a first set of FRAP experiments we analyzed the mobility of lamin C2-EGFP by bleaching an entire plaque at the NE and measured the fluorescence recovery in this area. For the control myr-lamin C-EGFP, a spot in the

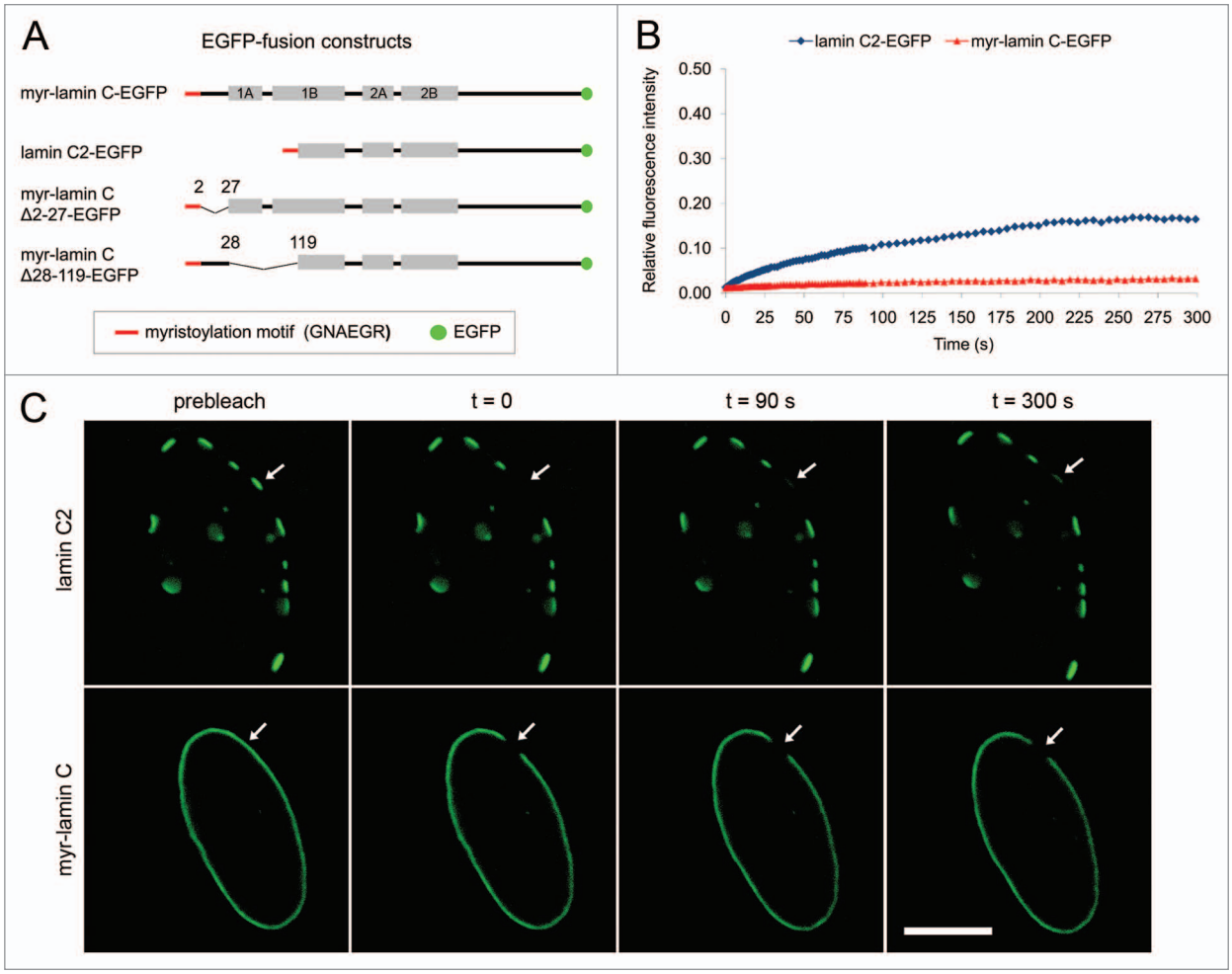

Figure 1. (A) Schematic overview of the used lamin C2- and lamin C-EGFP fusion constructs. Grey bars represent coils 1A, 1B, 2A and 2B of wild type lamin C. Meiosis-specific lamin C2 lacks the N-terminal head domain as well as coil 1A and a significant portion of coil 1B. EGFP not drawn to scale. (B) and (C) FRAP analysis of the mobility of lamin C2-EGFP and myr-lamin C-EGFP. A small area in the NE of 2 µm in diameter was bleached and the fluorescence recovery in this area was measured over time (arrows). For lamin C2-EGFP a plaque within the NE was bleached entirely. Scale bar, 10 µm.

NE of the same size was bleached. Consistent with earlier studies that analyzed the mobility of lamin C and other somatic lamins,[44-46] the fluorescence recovery of myr-lamin C-EGFP within the observed interval of 300 s was only marginal and occurred very slowly (~2%, n = 22, **Fig. 1B and C**), indicating that ectopic myristoylation did not alter the mobility of lamin C significantly. In contrast, the fluorescence of lamin C2-EGFP recovered considerably in the bleached area (~15%, n = 22, $p < 0.0001$, **Fig. 1B and C**). This data demonstrates that meiotic lamin C2 features a significantly increased mobility compared to lamin C and furthermore implicates that myristoylation of lamin C2 by itself cannot be a sufficient determinant of its increased mobility and unique localization pattern.

The role of the N-terminal truncation of lamin C2 for its unique localization and its dynamic properties. As myristoylation of lamin C2 turned out to be neither sufficient for its unique localization in discontinuous domains nor for its increased mobility, we analyzed the impact of the lacking N-terminal head and N-terminal portion of the α-helical rod domain on its specific properties. To address this issue we cloned two mutant lamin C-EGFP fusion constructs with an ectopic N-terminal myristoylation motif that lacked either the N-terminal globular head domain (myr-lamin CΔ2-27-EGFP) or the N-terminal portion of the α-helical rod domain (myr-lamin CΔ28-119-EGFP; see **Fig. 1A**). Interestingly, both lamin C deletion mutants localized at the NE in a pattern indistinguishable from that of lamin C2 (i.e., discrete plaques; **Fig. 2C**). Furthermore, as determined by photobleaching of entire plaques both lamin C deletion mutants showed a significantly increased mobility compared to myr-lamin C-EGFP (~13% for myr-lamin CΔ2-27-EGFP, n = 20, $p < 0.0001$, **Fig. 2A** and ~32% for myr-lamin CΔ28-119-EGFP, n = 21, $p < 0.0001$, **Fig. 2B**). Although the unexpectedly strong recovery of myr-lamin CΔ28-119-EGFP cannot be explained so far, our data nevertheless demonstrates that the lack of either the globular head domain (aa 2–27) or the N-terminal portion of the α-helical rod domain (aa 28–119) alone was sufficient to increase the mobility of lamin C up to a similar level observed for lamin C2 (~15%, compare **Fig. 1B**) or even beyond. Together,

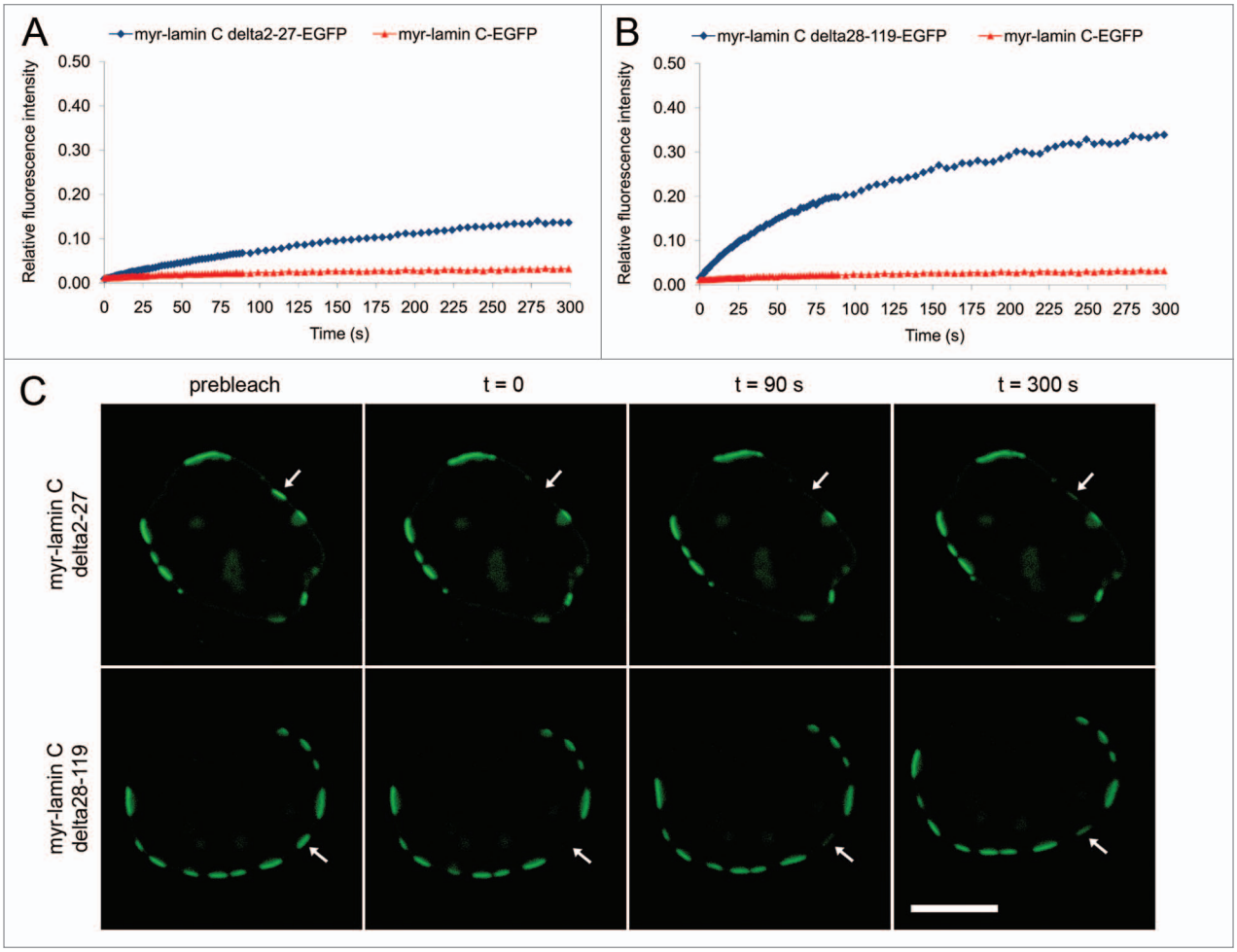

Figure 2. FRAP analysis of the mobility of lamin C-EGFP deletion mutants. Recovery curves of myr-lamin C Δ2-27-EGFP (A) and myr-lamin C Δ28-119-EGFP (B) were both compared to full length lamin C-EGFP. (C) Discrete plaques at the NE were bleached entirely with a spot of 2 μm in diameter (arrows). Scale bar, 10 μm.

our FRAP analyses of mutant lamin C proteins revealed that the N-terminal truncation of lamin C2 is a sufficient determinant for its localization in discrete domains and for its increased mobility.

High local mobility of lamin C2 within the discrete plaques. For all FRAP experiments described above the lamin C2 plaques were bleached entirely. Therefore, the observed fluorescence recoveries of the analyzed proteins could only be due to a more global exchange of molecules between the NE and a mobile fraction in the nucleoplasm and/or to lateral movement of molecules within the nuclear lamina between different plaques. Since not only in transfected cultured cells but also under in vivo conditions in spermatocytes, meiosis-specific lamin C2 is distributed in discontinuous domains at the NE, it seems reasonable to assume that the local mobility of lamin C2 within these discrete domains might be an important determinant for its physiological significance.[37] In order to analyze the local mobility of lamin C2, we performed further photobleaching experiments using a modified FRAP approach. Here only one half of a lamin C2 plaque was bleached and the recovery in this area was monitored. In addition, the loss of fluorescence in the unbleached part of the same plaque and the total fluorescence of the observed plaque as a whole was measured (**Fig. 3A**). Consistent with the data shown above, the total fluorescence of the partly bleached plaque recovered significantly within the observed interval of 90 s (~6%, n = 20, green curve in **Fig. 3B**), reflecting the previously described recovery of lamin C2-EGFP that we found when a plaque was bleached entirely. More importantly, the fluorescence of lamin C2-EGFP in the bleached half of the plaque recovered by ~29% (n = 20, yellow curve in **Fig. 3B**) within the same interval. Compared to the recoveries measured for myr-lamin C-EGFP (~0.5%, n = 21, $p < 0.0001$) and for lamin C2-EGFP when bleached as an entire plaque (~10%, n = 21, $p < 0.0001$), this recovery was much stronger. At the same time the fluorescence of the unbleached part of the same plaque rapidly decreased by ~22% (n = 20, red curve in **Fig. 3B**) indicating that most of the recovery in the bleached area was due to a pronounced lateral movement of lamin C2 molecules within the observed plaque. This data suggests that lamin C2 exhibits a very high local mobility within the discrete plaques which is even higher than the mobility we observed when we bleached an entire plaque.

To verify this observation, we used FLIP. Thereby, approximately one half of a single lamin C2 plaque was repeatedly

bleached and the fluorescence loss in the unbleached half of the same plaque was monitored over time. As controls, first we bleached an area in the NE located just adjacent to one discrete lamin C2 plaque and measured the fluorescence loss in this particular plaque. Second, we used myr-lamin C-EGFP as a further control where we performed bleaching and monitoring in the rim-like pattern within the NE in an analogue way (**Fig. 4A**). To exclude the possibility that differences in the observed fluorescence losses were due to varying distances between the bleached and the monitored area, these distances were standardized to approximately 1 µm for all measurements. As expected, the fluorescence loss of myr-lamin C-EGFP was very low in the observed interval of 150 s (~7%, n = 20, blue curve in **Fig. 4B**), reflecting the only marginal mobility of lamin C already defined by FRAP. Similarly, for lamin C2-EGFP, the fluorescence of a monitored plaque only decreased slightly within 150 s when we bleached an area adjacent to that particular plaque (~10%, n = 20, yellow curve in **Fig. 4B**), suggesting that the mobility of lamin C2 within the NE between the discrete plaques is not very pronounced. In contrast, when half of a lamin C2 plaque was repeatedly bleached the fluorescence in the unbleached half of this particular plaque rapidly decreased by ~63% within the same interval (n = 20, $p < 0.0001$ compared to either of the controls, red curve in **Fig. 4B**). These results clearly confirm that meiosis-specific lamin C2 is very mobile within the discrete domains formed at the NE.

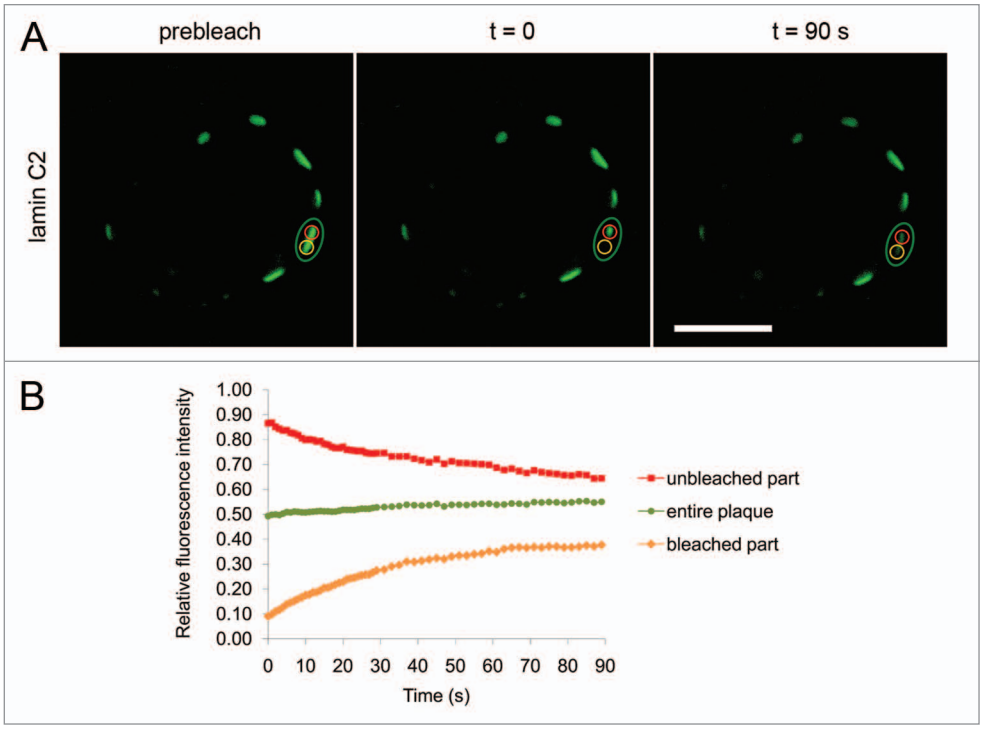

Figure 3. FRAP analysis of the mobility of lamin C2-EGFP within the discrete plaques. (A) Half of a plaque was bleached with a spot of 2 µm in diameter and the fluorescence recovery in this area was monitored over time (yellow ROI). At the same time, the fluorescence in the unbleached half of this particular plaque (red ROI) as well as the fluorescence of the observed plaque as a whole (green ROI) was measured. Scale bar, 10 µm. (B) Quantification of FRAP experiment depicted in (A). Colouring of curves corresponds to the ROIs described above.

Ectopic expression of meiosis-specific lamin C2 induces nuclear deformations and alters the distribution of endogenous NE proteins. The photobleaching experiments described above strongly suggest that meiosis-specific lamin C2 is in fact able to modulate the physical properties of the NE by means of its significantly increased mobility. To confirm this modulation on a rather structural level, we additionally performed immunolocalization experiments. Here, we analyzed potential alterations of nuclear morphology and possible redistributions of endogenous NE proteins induced by the ectopic expression of lamin C2-EGFP in somatic cells. To mimic the composition of the nuclear lamina (i.e., absence of lamins A/C) of the natural meiotic environment of lamin C2 in male meiotic germ cells (i.e., spermatocytes), our immunolocalization experiments again were performed in *Lmna*$^{-/-}$ MEFs.[29,42] Noteworthy, all of the analyzed endogenous proteins (lamin B1, LAP2, SUN1 and SUN2) have previously been shown to be present in the NE of spermatocytes.[29,47-49] Therefore their expression is temporally and spatially associated with the emergence of lamin C2 in vivo. Moreover, in mammalian spermatocytes SUN1 and SUN2 were found to be localized at the sites of NE attachment of meiotic telomeres,[48,49] suggesting that a functional association of these proteins with lamin C2 might also be present and physiologically significant under meiotic conditions in vivo.

With regard to nuclear shape most non-transfected *Lmna*$^{-/-}$ MEFs as well as control cells transfected with myr-lamin C-EGFP exhibited round or oval nuclei. Consistent with previous reports,[42,50] a fraction of non-transfected *Lmna*$^{-/-}$ MEFs (34%, n = 659) featured nuclei with aberrant morphology (i.e., deviation from a round or ovoid shape), which was most probably due to the reduced mechanical resistance resulting from the loss of lamins A/C already described earlier.[51] In control cells expressing myr-lamin C-EGFP the ratio of aberrant nuclei was similar (41%, n = 264, $p = 0.042$ compared to non-transfected cells). In clear contrast, the vast majority of nuclei in cells expressing lamin C2-EGFP showed significant morphological alterations in terms of a multi-curved shape (82%, n = 204, $p < 0.0001$ compared to either of the controls; see also **Figs. 5–8**).

To more directly investigate the effect of the expression of lamin C2 on the NE we analyzed the distribution of endogenous lamin B1. As expected, in non-transfected *Lmna*$^{-/-}$ MEFs lamin B1 localized in a homogenous rim-like pattern at the NE (**Fig. 5A–A'''**). In cells expressing myr-lamin C-EGFP the

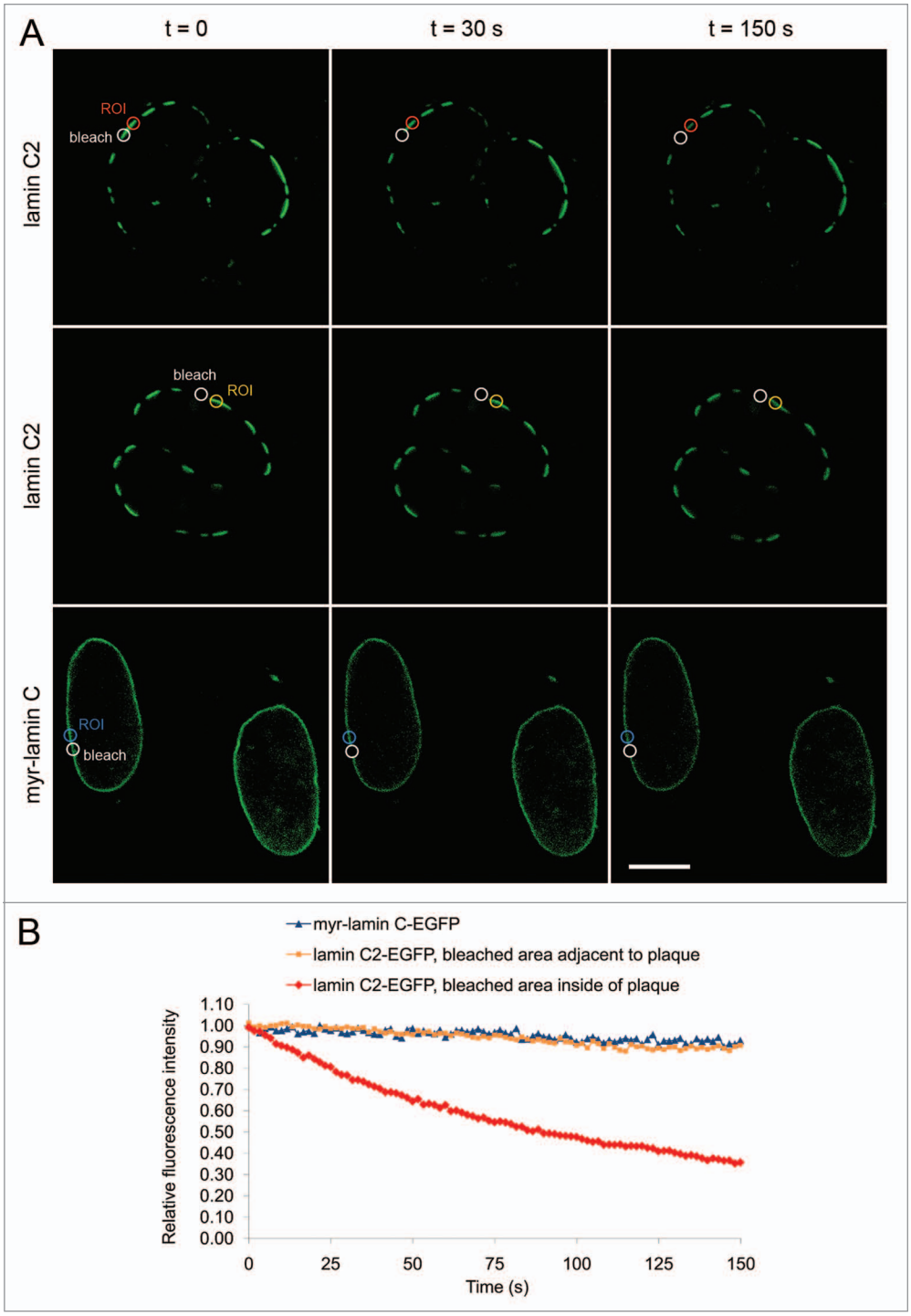

Figure 4. FLIP analysis of the mobility of lamin C2-EGFP within the discrete plaques. (A) upper row: Half of a discrete plaque at the NE was repeatedly bleached with a small spot of a 1µm in diameter (white "bleach"). The fluorescence loss in the unbleached half of the same plaque was monitored over time (red "ROI"). As a control, a spot of the same size just adjacent to one particular plaque was bleached and the fluorescence loss of this plaque was monitored (middle row; yellow "ROI"). As a further control, an area of appropriate size was bleached within the continuous rim-like pattern of myr-lamin C-EGFP and the fluorescence loss next to this area was measured (lower row; blue "ROI"). Scale bar, 10 µm. (B) Quantification of the FLIP experiment depicted in (A). Colouring of curves corresponds to the ROIs described above.

localization of lamin B1 was indistinguishable from non-transfected ones (**Fig. 5C–C'''**). Interestingly, the expression of lamin C2-EGFP induced considerable redistributions of lamin B1. Here, the rim-like staining of lamin B1 was less homogenous and local maxima of lamin B1 often co-localized with the discrete lamin C2 plaques (**Fig. 5B–B'''**).

Since nuclear lamins are known to interact with several NE proteins of the INM, we additionally analyzed the distribution

of some lamin-binding INM proteins (LAP2, SUN1 and SUN2) in *Lmna*$^{-/-}$ MEFs ectopically expressing lamin C2.[5] In non-transfected cells all three analyzed endogenous NE proteins localized in a continuous rim-like pattern at the NE (**Figs. 6A–A'''; 7A–A'''; 8A–A'''**). In *Lmna*$^{-/-}$ MEFs transfected with myr-lamin C-EGFP the localization of LAP2, SUN1 and SUN2 was not altered significantly compared to non-transfected cells (**Figs. 6C–C'''; 7C–C'''; 8C–C'''**). Interestingly, the expression of lamin C2-EGFP induced considerable redistributions of all analyzed NE proteins. The distribution of LAP2 (**Fig. 6B–B'''**) and SUN2 (**Fig. 8B–B'''**) was changed in a similar manner described above for lamin B1. Additionally, SUN2 partly localized in cytoplasmic aggregates. The most pronounced effect, however, was seen for SUN1 (**Fig. 7B–B'''**). Here, the staining at the NE was severely fragmented and a significant portion of the protein was displaced into the cytoplasm.

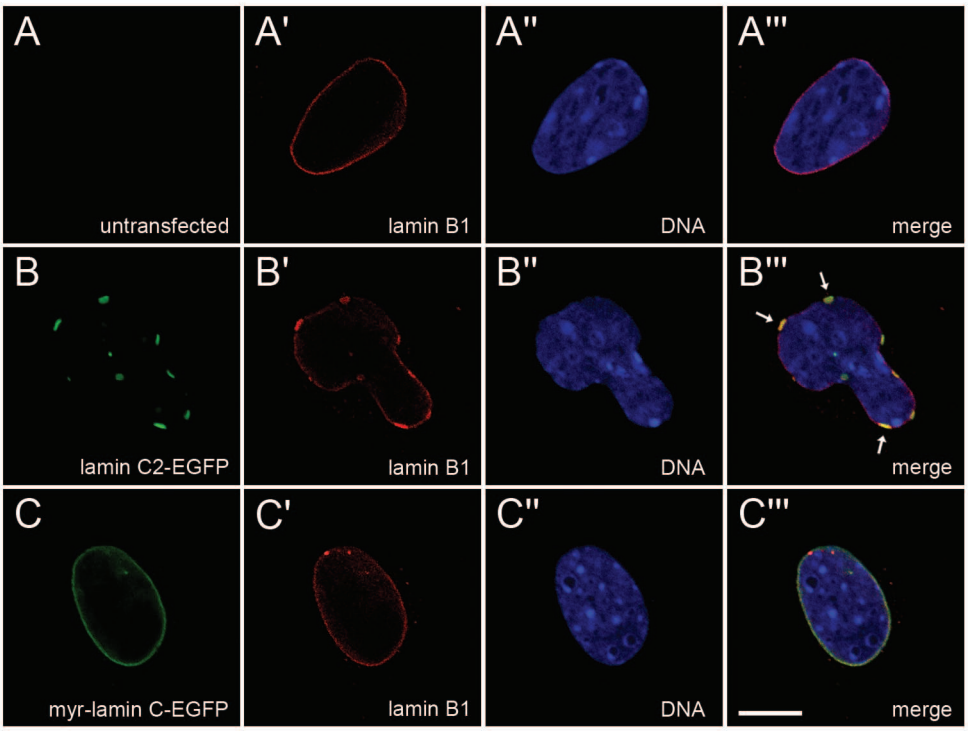

Figure 5. The distribution of endogenous lamin B1 was detected with mAb 119D5-F1 in non-transfected (A–A''') *Lmna*$^{-/-}$ MEFs as well as in cells transfected with either lamin C2-EGFP (B–B''') or myr-lamin C-EGFP (C–C'''). DNA was stained with Hoechst-33258. To ensure equivalent experimental conditions, non-transfected cells (as judged by the absence of EGFP-fluorescence) were selected from the vicinity of cells expressing lamin C2-EGFP or myr-lamin C-EGFP on the same coverslip. Arrows in (B''') indicate co-localization of local maxima of lamin B1 with plaques formed by lamin C2-EGFP. Scale bar, 10 µm.

In summary, these immunolocalization experiments revealed a considerable modulation of nuclear morphology and an altered spatial arrangement of endogenous NE proteins induced by the ectopic expression of lamin C2 in somatic cells.

Discussion

Lamin C2 is a short splice variant of the *Lmna* gene which is selectively expressed during meiotic stages of spermatogenesis (i.e., in spermatocytes).[32-34] Compared to somatic lamins it features an N-terminal myristoylation motif instead of a C-terminal farnesylation signal and therefore differs concerning its targeting to the NE.[36] Furthermore, it lacks the globular head and a significant portion of the α-helical rod domain present in somatic lamins.[33,34] Since these domains are known to be critically involved in lamin assembly, it has been postulated that the presence of lamin C2 in the nuclear lamina meshwork modulates the structural integrity of the NE, thus providing unique physiological features to the NE of spermatocytes required for meiosis-specific events.[10,18,19,34,37]

In our present study this issue was experimentally addressed by several photobleaching and immunolocalization approaches. Our results demonstrate that (1) the expression of lamin C2 in somatic cells induced an aberrant nuclear morphology and altered the distribution of endogenous NE proteins. (2) Compared to its somatic counterpart lamin C, meiosis-specific lamin C2 features a significantly increased mobility, which is (3) most pronounced within the discrete plaques of lamin C2 formed at the NE. A further important aspect of our experiments was the finding, that (4) either the deletion of the N-terminal head or the N-terminal portion of the α-helical rod domain of lamin C alone was sufficient to induce a lamin C2-like distribution (i.e., formation of discrete plaques at the NE) and to raise the mobility of the resulting proteins up to the level observed for lamin C2 or even beyond. In contrast, we could not find any evidence that ectopic myristoylation of lamin C per se induced physiological properties differing from somatic lamins (i.e., localization in a homogenous rim-like pattern at the NE and virtual immobility). Thus, we conclude that the N-terminal truncation rather than myristoylation is the primary determinant of the unique localization of meiosis-specific lamin C2 in discrete plaques and of its increased mobility.

This notion is in line with previous studies analyzing the roles of the globular head and the α-helical rod domain of lamins for their polymer assembly and their physiological properties. Particularly, Schirmer and colleagues reported that the expression of a mutant human lamin B1 lacking the central four-fifths of the α-helical rod domain induced severe nuclear deformations and altered the distribution of endogenous lamins and other NE proteins.[52] Interestingly, mutant lamin B1 was distributed in discontinuous domains. Furthermore, it showed significantly weakened heterotypic interactions with wild-type lamins which were

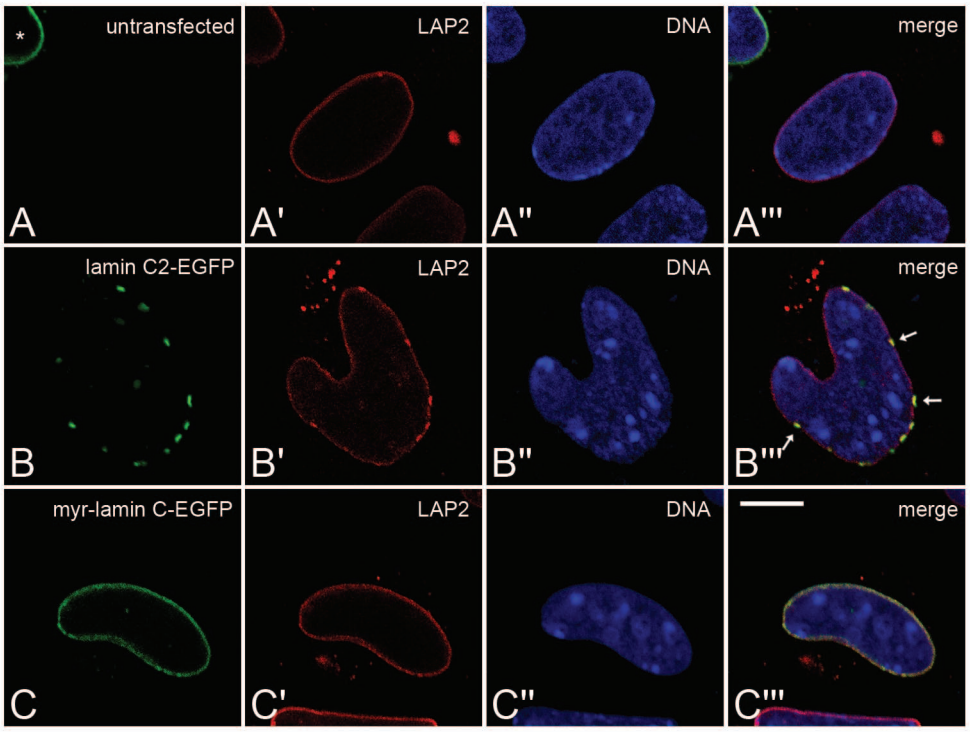

Figure 6. The distribution of endogenous LAP2 isoforms was detected with mAb 13d4 (recognizing all major LAP2 isoforms; ref. 47) in non-transfected (A–A''') *Lmna*$^{-/-}$ MEFs as well as in cells transfected with either lamin C2-EGFP (B–B''') or myr-lamin C-EGFP (C–C'''). DNA was stained with Hoechst-33258. To ensure equivalent experimental conditions, non-transfected cells (as judged by the absence of EGFP-fluorescence) were selected from the vicinity of cells expressing lamin C2-EGFP or myr-lamin C-EGFP on the same coverslip. Asterisk in (A) indicates a myr-lamin C-EGFP expressing cell in close vicinity to the untransfected control cell (no EGFP fluorescence) located in middle of the panel. Arrows in (B''') indicate co-localization of local maxima of LAP2 with plaques formed by lamin C2-EGFP. Scale bar, 10 µm.

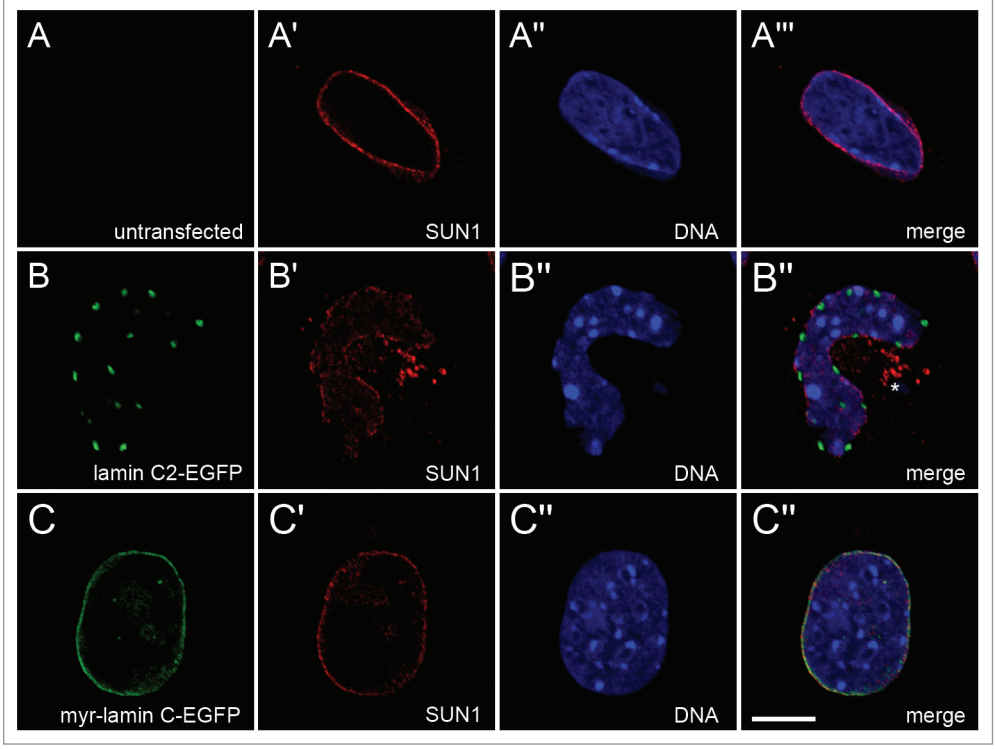

interpreted as the biochemical cause for the observed morphological changes. Another study reported a significant reduction of the homotypic binding strength of the same lamin B1 mutant (lacking four-fifths of the α-helical rod) as well as for a corresponding human lamin C mutant.[53] With regard to this, we propose that meiosis-specific lamin C2 can be considered as a "natural lamin C deletion mutant" lacking a smaller yet significant portion of the α-helical rod. Thus, similar reductions of homotypic and/or heterotypic lamin interactions could account for the altered nuclear morphology in lamin C2 expressing somatic cells and the increased mobility of lamin C2 we observed in our experiments. Further studies analyzing the role of the globular lamin head for lamin polymer assembly showed that this domain is critically involved in head-to-tail associations of dimers.[54,55] Moreover, Moir and colleagues reported an increased solubility of a human lamin C mutant lacking the N-terminal globular head.[56] Taken together, both the globular head as well as the α-helical rod domain of nuclear lamins were found to be critical determinants of the stability and structure of lamin polymers. In our present study this notion is reflected in the finding that the deletion of either of these domains was sufficient to significantly increase the mobility

Figure 7. The distribution of endogenous SUN1 was detected with guinea pig pAb in non-transfected (A–A''') *Lmna*$^{-/-}$ MEFs as well as in cells transfected with either lamin C2-EGFP (B–B''') or myr-lamin C-EGFP (C–C'''). DNA was stained with Hoechst-33258. To ensure equivalent experimental conditions, non-transfected cells (as judged by the absence of EGFP-fluorescence) were selected from the vicinity of cells expressing lamin C2-EGFP or myr-lamin C-EGFP on the same coverslip. Asterisk in (B''') indicates cytoplasmic aggregates of SUN1. Scale bar, 10 µm.

of lamin C in FRAP experiments and to induce an altered distribution (i.e., formation of discrete plaques).

In vertebrate germ cells lamin C2 is not the only naturally occurring lamin variant exhibiting an altered domain structure compared to somatic counterparts. Similar to the data presented in this study for meiosis-specific lamin C2, the N-terminally truncated spermiogenesis-specific (i.e., post-meiotic) murine lamin B3 has been shown to feature physiological properties different from somatic lamins, including the induction of nuclear deformations in somatic cells, an increased biochemical extractability and an increased mobility in photobleaching studies.[31,35,57] Importantly, all these features of lamin B3 could be clearly ascribed to the truncation of the α-helical rod domain.[57] Moreover, a recent study reported that human lamin B3 failed to assemble into bona fide lamin filaments when expressed in Xenopus oocytes.[58] Another male germ cell-specific lamin, lamin LIV, is present in the amphibian *Xenopus laevis* during post-meiotic stages of spermatogenesis and has recently been characterized on the molecular level in closer detail.[58,59] Here, it was found that in contrast to the truncated mammalian lamins C2 and B3, Xenopus lamin LIV exhibits an extra sequence of 40 amino acids within the central α-helical rod that was predicted to impede coiled-coil formation.[58] Consistent with that, lamin LIV failed to assemble into bona fide filaments when expressed in Xenopus oocytes. Consequently, it was suggested that Xenopus lamin LIV and mammalian lamin B3 fulfill similar physiological functions.

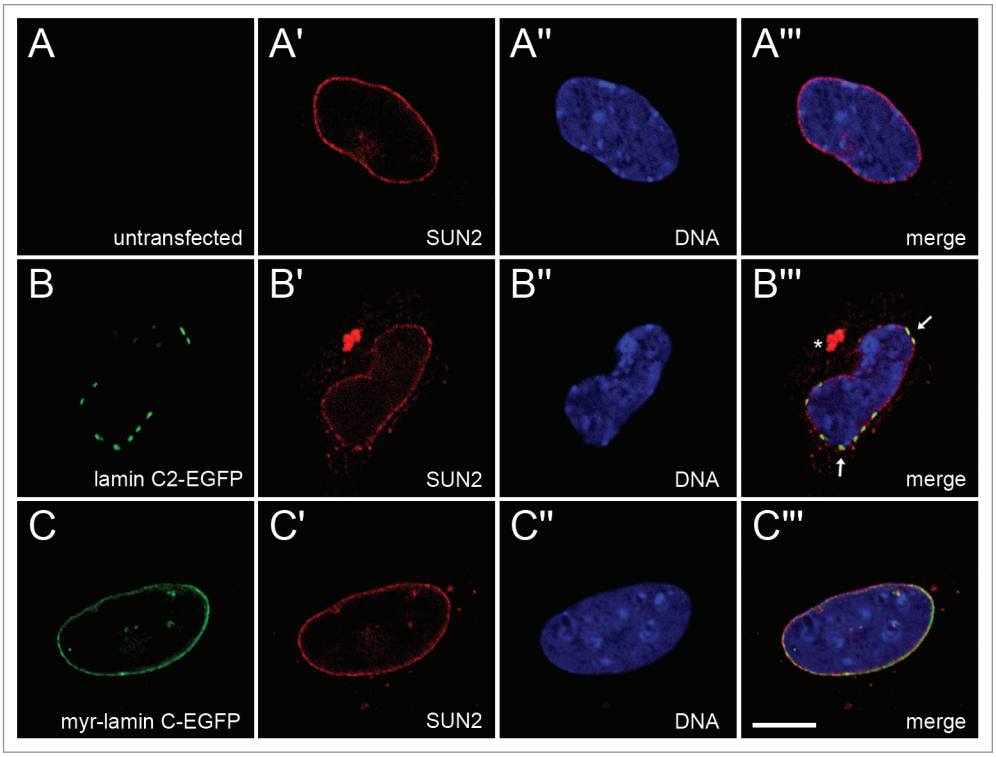

Figure 8. The distribution of endogenous SUN2 was detected with rabbit pAb in non-transfected (A–A‴) *Lmna*$^{-/-}$ MEFs as well as in cells transfected with either lamin C2-EGFP (B–B‴) or myr-lamin C-EGFP (C–C‴). DNA was stained with Hoechst-33258. To ensure equivalent experimental conditions, non-transfected cells (as judged by the absence of EGFP-fluorescence) were selected from the vicinity of cells expressing lamin C2-EGFP or myr-lamin C-EGFP on the same coverslip. Arrows in (B‴) indicate co-localization of local maxima of SUN2 with plaques formed by lamin C2-EGFP. Cytoplasmic aggregation of SUN2 is indicated by asterisk. Scale bar, 10 μm.

Germ cell-specific lamin variants feature striking similarities concerning their altered domain organization compared to somatic lamins and their properties in vitro. Mammalian lamin B3 and Xenopus lamin LIV are present during post-meiotic stages of spermatogenesis when yet haploid cell nuclei undergo profound morphological and functional reorganizations.[60,61] In contrast, lamin C2 is selectively expressed during meiotic stages of spermatogenesis and therefore encounters a completely different cellular environment. A most central feature of meiotic prophase I are the dynamic telomere-driven chromosome movements including the formation and resolution of the chromosomal bouquet during early stages as well as ongoing oscillatory chromosome movements during mid-prophase I. These movements are considered to be crucial for proper pairing and synapsis of the homologous chromosomes. They, in turn, require tethering of the meiotic telomeres to the NE and their subsequent lateral movement at the plane of the NE.[38-41] In mammals the sites of telomere attachment were found to be embedded in the discontinuous domains formed by lamin C2.[37] With regard to this spatial relation and the peculiarities of lamin C2 concerning its domain structure it was hypothesized that lamin C2 modulates the structural integrity of the NE at the sites of telomere attachment and therefore allows for their proper attachment and/or dynamic repositioning.[34,37] In our present study we provide first direct experimental evidence strongly supporting this notion. Moreover, based on our data described above, we present a more precise picture of the molecular properties of meiosis-specific lamin C2. Our findings suggest that due to its increased mobility and its impact on other NE proteins the discontinuous domains of lamin C2 found at the NE of mammalian spermatocytes can be considered as dynamic platforms exhibiting a significantly reduced mechanical stiffness that enable meiotic telomeres to slide at the plane of the nuclear envelope.

Materials and Methods

Cloning of EGFP fusion constructs. To express EGFP fusion proteins in cultured mammalian cells cDNAs coding for the proteins of interest were cloned into mammalian expression vector

pEGFP-N2 (Clontech, Heidelberg, Germany). To this end, total RNA was isolated from mouse testis and served as a template to produce total cDNA by reverse transcription using oligo-dT primers (Fermentas). The sequences coding for murine lamin C2 (GeneBank accession number NM_019390) and murine lamin C (GeneBank accession number NM_001111102) were amplified by PCR with specific primers (lamin C2 5', lamin C 5', lamin C2/C 3', see **Suppl. Table**).[33,43] The resulting DNA fragments were subcloned into vector pCR2.1-TOPO (Invitrogen) and used as templates to eliminate stop codons by PCR mutagenesis (primers were lamin C2 5' and lamin C2/C TAA-3' for lamin C2). Additionally for myr-lamin C, 18 nucleotides coding for the N-terminal myristoylation motif (GNAEGR) of wild-type lamin C2 were added to the 5'-end of the lamin C coding sequence by PCR mutagenesis in two subsequent steps (first step 5', second step 5' and lamin C2/C TAA-3').[36] The resulting PCR products were again subcloned into vector pCR2.1-TOPO and finally ligated into vector pEGFP-N2 using EcoRI restriction sites. Furthermore, two lamin C deletion mutants (myr-lamin CΔ2-27-EGFP and myr-lamin CΔ28-119-EGFP) lacking the globular head domain (aa 2–27) and the N-terminal portion of the α-helical rod domain (aa 28–119), respectively, were constructed by PCR mutagenesis with inverted primer pairs flanking the deletions (primers were Δ2-27 5', Δ2-27 3' and Δ28-119 5', Δ28-119 3'). Here, plasmid myr-lamin C-EGFP was used as a template. The resulting PCR products were ligated to form functional plasmids.

Cell culture and transfection. *Lmna*$^{-/-}$ MEFs were cultured in DMEM Glutamax (Gibco) with 10% (v/v) FCS, 1% (v/v) Penicillin/Streptomycin and 1% (v/v) L-Glutamin at 37°C and 5% CO_2.[42] 18–24 h before further treatment, cells were transiently transfected using MATra (IBA, Göttingen, Germany) and 2 µg of plasmid DNA as specified by the manufacturer.

Immunofluorescence microscopy. Primary antibodies were mAb 119D5-F1 (Santa Cruz Biotechnology) against lamin B1 (1:100), guinea pig pAb against SUN1 (1:800), rabbit pAb against SUN2 (1:50) and mAb 13d4 recognizing all major LAP2 isoforms (undiluted).[47,62] Secondary antibodies were goat anti-mouse IgG/M-TexasRed, goat anti-guinea pig IgG/M-TexasRed and goat anti-rabbit IgG-TexasRed (1:50 each; Dianova, Hamburg, Germany).

For immunolocalization of endogenous NE proteins, transiently transfected cells grown on coverslips were rinsed with PBS (140 mM NaCl, 2.6 mM KCl, 6.4 mM Na_2HPO_4, 1.4 mM KH_2PO_4, pH 7.4), fixed with 1% formaldehyde in PBS (3 min) and permeabilized with 0.1% Triton X-100 in PBS (5 min). After washing with PBS (3 x 5 min) cells were blocked with PBT (PBS, 1.5% BSA, 0.1% Tween-20) for 1 h. Samples were successively incubated with primary and secondary antibodies for 30 min each. Each incubation step was followed by washing with PBS (3 x 5 min). Additionally, during secondary antibody incubation DNA was stained with Hoechst-33258 for 10 min. Cells were finally embedded in Glycerin-PBS (1:1) and analyzed by confocal microscopy on a Leica TCS-SP2. The three used fluorochromes (Hoechst-33258, EGFP, TexasRed) were scanned sequentially using appropriate laser settings for each channel (Hoechst-33258: excitation 405 nm, detection 415–480 nm; EGFP: excitation 488 nm, detection 500–575 nm; TexasRed: excitation 561 nm; detection 600–700 nm). Single section scans were taken with a 63x/1.40 HCX PL APO lbd.BL oil-immersion objective, pinhole at 1.00 P AU and 4x accumulation. Three sequenced single section scans of each channel were used to calculate the maximum 2D projection using the Leica TCS-SP2 microscope software. Image data was edited with Adobe Photoshop.

To quantify aberrations of nuclear morphology induced by the expression of lamin C2 in somatic cells, nuclear shape was classified according to Lammerding and colleagues as normal (i.e., round or ovoid) or aberrant (i.e., deviation from a round or ovoid shape) as judged by means of the Hoechst-33258 fluorescence.[50] The ratio of aberrantly shaped nuclei was calculated for non-transfected cells as well as for cells expressing either lamin C2-EGFP or myr-lamin C-EGFP and the statistical significance was determined with a chi-square test.

FRAP and FLIP analyses. Live-cell imaging of transiently transfected cells was performed in FluoroDish culture dishes (World Precision Instruments, Sarasota, USA) under culture conditions (37°C, 5% CO_2) on a Leica TCS-SP2 confocal laser scanning microscope using the 488 nm laser line of an Ar/Kr laser (6 mW nominal output, 63x/1.40 HCX PL APO lbd.BL oil-immersion objective, pinhole setting 1.60 P AU, detection 500–575 nm). For FRAP experiments, two single scans were acquired, followed by eight bleach pulses of 0.837 s without scanning using a bleach spot of 2 µm in radius. Single section images with 2x accumulation were collected at 1 s (30 images), 2 s (30 images) and 5 s intervals (42 images). For imaging, laser power was attenuated to 7% of bleach intensity. For FLIP experiments, cells were repeatedly bleached and imaged at intervals of 0.837 s (91 images) with 2x accumulation and a bleach spot of 1 µm in radius. For imaging, laser power was attenuated to 5% of bleach intensity. FRAP and FLIP curves were generated with Microsoft Excel from background subtracted images according to Phair and Misteli.[63] To quantitatively compare the fluorescence recoveries of the analyzed proteins in FRAP experiments, recoveries were calculated as $FRAP = I_{rel}(end) - I_{rel}(0)$ with $I_{rel}(end)$ being the relative fluorescence intensity at the end of the observed interval and $I_{rel}(0)$ being the intensity directly after bleaching. For FLIP, the fluorescence losses were calculated as $FLIP = I_{rel}(0) - I_{rel}(end)$ with $I_{rel}(0)$ being the fluorescence directly before the first bleach pulse. The statistical significance of FRAP and FLIP values was verified by Student's t-test.

Acknowledgements

Lmna$^{-/-}$ MEFs were kindly provided by Colin L. Stewart and Roland Foisner. This work was supported by the Graduate School GK 1048 "Molecular basis of organ development in vertebrates" (TP A1), the Elitenetzwerk Bayern and grants Al 1090/1-1 and SPP1384 of Deutsche Forschungsgemeinschaft to M. A.

Note

Supplementary materials can be found at:
www.landesbioscience.com/supplement/JahnNUC1-3-Sup.pdf

References

1. McKeon FD, Kirschner MW, Caput D. Homologies in both primary and secondary structure between nuclear envelope and intermediate filament proteins. Nature 1986; 319:463-8.
2. Fisher DZ, Chaudhary N, Blobel G. cDNA sequencing of nuclear lamins A and C reveals primary and secondary structural homology to intermediate filament proteins. Proc Natl Acad Sci USA 1986; 83:6450-4.
3. Hutchison CJ. Lamins: building blocks or regulators of gene expression? Nat Rev Mol Cell Biol 2002; 3:848-58.
4. Gruenbaum Y, Margalit A, Goldman RD, Shumaker DK, Wilson KL. The nuclear lamina comes of age. Nat Rev Mol Cell Biol 2005; 6:21-31.
5. Schirmer EC, Foisner R. Proteins that associate with lamins: many faces, many functions. Exp Cell Res 2007; 313:2167-79.
6. Burke B, Stewart CL. Life at the edge: the nuclear envelope and human disease. Nat Rev Mol Cell Biol 2002; 3:575-85.
7. Cohen TV, Hernandez L, Stewart CL. Functions of the nuclear envelope and lamina in development and disease. Biochem Soc Trans 2008; 36:1329-34.
8. Krohne G, Benavente R. The nuclear lamins: a multigene family of proteins in evolution and differentiation. Exp Cell Res 1986; 162:1-10.
9. Nigg EA. The nuclear envelope. Curr Opin Cell Biol 1989; 1:435-40.
10. Stuurman N, Heins S, Aebi U. Nuclear lamins: their structure, assembly and interactions. J Struct Biol 1998; 122:42-66.
11. Höger TH, Krohne G, Franke WW. Amino acid sequence and molecular characterization of murine lamin B as deduced from cDNA clones. Eur J Cell Biol 1988; 47:283-90.
12. Zewe M, Höger TH, Fink T, Lichter P, Krohne G, Franke WW. Gene structure and chromosomal localization of the murine lamin B2 gene. Eur J Cell Biol 1991; 56:342-50.
13. Stewart C, Burke B. Teratocarcinoma stem cells and early mouse embryos contain only a single major lamin polypeptide closely resembling lamin B. Cell 1987; 51:383-92.
14. Lin F, Worman HJ. Structural organization of the human gene encoding nuclear lamin A and nuclear lamin C. J Biol Chem 1993; 268:16321-6.
15. Röber RA, Weber K, Osborn M. Differential timing of nuclear lamin A/C expression in the various organs of the mouse embryo and the young animal: a developmental study. Development 1989; 105:365-78.
16. Dhe-Paganon S, Werner ED, Chi YI, Shoelson SE. Structure of the globular tail of nuclear lamin. J Biol Chem 2002; 277:17381-4.
17. Krimm I, Östlund C, Gilquin B, Couprie J, Hossenlopp P, Mornon JP, et al. The Ig-like structure of the C-terminal domain of lamin A/C, mutated in muscular dystrophies, cardiomyopathy, and partial lipodystrophy. Structure 2002; 10:811-23.
18. Krohne G. Lamin assembly in vivo. Subcell Biochem 1998; 31:563-86.
19. Herrmann H, Aebi U. Intermediate filaments: molecular structure, assembly mechanism and integration into functionally distinct intracellular scaffolds. Annu Rev Biochem 2004; 73:749-89.
20. Loewinger L, McKeon F. Mutations in the nuclear lamin proteins resulting in their aberrant assembly in the cytoplasm. EMBO J 1988; 7:2301-9.
21. Holtz D, Tanaka RA, Hartwig J, McKeon F. The CaaX motif of lamin A functions in conjunction with the nuclear localization signal to target assembly to the nuclear envelope. Cell 1989; 59:969-77.
22. Krohne G, Waizenegger I, Höger TH. The conserved carboxy-terminal cysteine of nuclear lamins is essential for lamin association with the nuclear envelope. J Cell Biol 1989; 109:2003-11.
23. Kitten GT, Nigg EA. The CaaX motif is required for isoprenylation, carboxyl methylation, and nuclear membrane association of lamin B2. J Cell Biol 1991; 113:13-23.
24. Young SG, Fong LG, Michaelis S. Prelamin A, Zmpste24, misshapen cell nuclei, and progeria—new evidence suggesting that protein farnesylation could be important for disease pathogenesis. J Lipid Res 2005; 46:2531-58.
25. Weber K, Plessmann U, Traub P. Maturation of nuclear lamin A involves a specific carboxy-terminal trimming, which removes the polyisoprenylation site from the precursor; implications for the structure of the nuclear lamina. FEBS Lett 1989; 257:411-4.
26. Horton H, McMorrow I, Burke B. Independent expression and assembly properties of heterologous lamins A and C in murine embryonal carcinomas. Eur J Cell Biol 1992; 57:172-83.
27. Ye Q, Worman HJ. Protein-protein interactions between human nuclear lamins expressed in yeast. Exp Cell Res 1995; 219:292-8.
28. Pugh GE, Coates PJ, Lane EB, Raymond Y, Quinlan RA. Distinct nuclear assembly pathways for lamins A and C lead to their increase during quiescence in Swiss 3T3 cells. J Cell Sci 1997; 110:2483-93.
29. Vester B, Smith A, Krohne G, Benavente R. Presence of a nuclear lamina in pachytene spermatocytes of the rat. J Cell Sci 1993; 104:557-63.
30. Nakajima N, Abe K. Genomic structure of the mouse A-type lamin gene locus encoding somatic and germ cell-specific lamins. FEBS Lett 1995; 365:108-14.
31. Furukawa K, Hotta Y. cDNA cloning of a germ cell specific lamin B3 from mouse spermatocytes and analysis of its function by ectopic expression in somatic cells. EMBO J 1993; 12:97-106.
32. Smith A, Benavente R. Identification of a short nuclear lamin protein selectively expressed during meiotic stages of rat spermatogenesis. Differentiation 1992; 52:55-60.
33. Furukawa K, Inagaki H, Hotta Y. Identification and cloning of an mRNA coding for a germ cell-specific A-type lamin in mice. Exp Cell Res 1994; 212:426-30.
34. Alsheimer M, Benavente R. Change of karyoskeleton during mammalian spermatogenesis: expression pattern of nuclear lamin C2 and its regulation. Exp Cell Res 1996; 228:181-8.
35. Schütz W, Alsheimer M, Öllinger R, Benavente R. Nuclear envelope remodeling during mouse spermiogenesis: postmeiotic expression and redistribution of germline lamin B3. Exp Cell Res 2005; 307:285-91.
36. Alsheimer M, von Glasenapp E, Schnölzer M, Heid H, Benavente R. Meiotic lamin C2: the unique amino-terminal hexapeptide GNAEGR is essential for nuclear envelope association. Proc Natl Acad Sci USA 2000; 97:13120-5.
37. Alsheimer M, von Glasenapp E, Hock R, Benavente R. Architecture of the nuclear periphery of rat pachytene spermatocytes: distribution of nuclear envelope proteins in relation to synaptonemal complex attachment sites. Mol Biol Cell 1999; 10:1235-45.
38. Scherthan H, Weich S, Schwegler H, Heyting C, Härle M, Cremer T. Centromere and telomere movements during early meiotic prophase of man and mouse are associated with the onset of chromosome pairing. J Cell Biol 1996; 134:1109-25.
39. Zickler D, Kleckner N. The leptotene-zygotene transition of meiosis. Annu Rev Genet 1998; 32:619-97.
40. Alsheimer M. The dance floor of meiosis: evolutionary conservation of nuclear envelope attachment and dynamics of meiotic telomeres. In: Benavente R, Volff JN, eds. Genome Dynamics. Basel: Karger 2009; 81-93.
41. Koszul R, Kleckner N. Dynamic chromosome movements during meiosis: a way to eliminate unwanted connections? Trends Cell Biol 2009; 19:716-24.
42. Sullivan T, Escalante-Alcalde D, Bhatt H, Anver M, Bhat N, Nagashima K, et al. Loss of A-type lamin expression compromises nuclear envelope integrity leading to muscular dystrophy. J Cell Biol 1999; 147:913-9.
43. Riedel W, Werner D. Nucleotide sequence of the full-length mouse lamin C cDNA and its deduced amino-acid sequence. Biochim Biophys Acta 1989; 1008:119-22.
44. Broers JL, Machiels BM, van Eys GJ, Kuijpers HJ, Manders EM, van Driel R, et al. Dynamics of the nuclear lamina as monitored by GFP-tagged A-type lamins. J Cell Sci 1999; 112:3463-75.
45. Moir RD, Yoon M, Khuon S, Goldman RD. Nuclear lamins A and B1: different pathways of assembly during nuclear envelope formation in living cells. J Cell Biol 2000; 151:1155-68.
46. Gilchrist S, Gilbert N, Perry P, Ostlund C, Worman HJ, Bickmore WA. Altered protein dynamics of disease-associated lamin A mutants. BMC Cell Biol 2004; 5:46-54.
47. Alsheimer M, Fecher E, Benavente R. Nuclear envelope remodelling during rat spermiogenesis: distribution and expression pattern of LAP2/thymopoietins. J Cell Sci 1998; 111:2227-34.
48. Ding X, Xu R, Yu J, Xu T, Zhuang Y, Han M. SUN1 is required for telomere attachment to nuclear envelope and gametogenesis in mice. Dev Cell 2007; 12:863-72.
49. Schmitt J, Benavente R, Hodzic D, Höög C, Stewart CL, Alsheimer M. Transmembrane protein Sun2 is involved in tethering mammalian meiotic telomeres to the nuclear envelope. PNAS 2007; 104:7426-31.
50. Lammerding J, Fong LG, Ji JY, Reue K, Stewart CL, Young SG, et al. Lamins A and C but not lamin B1 regulate nuclear mechanics. J Biol Chem 2006; 281:25768-80.
51. Broers JL, Peeters EA, Kuijpers HJ, Endert J, Bouten CV, Oomens CW, et al. Decreased mechanical stiffness in LMNA$^{-/-}$ cells is caused by defective nucleo-cytoskeletal integrity: implications for the development of laminopathies. Hum Mol Genet 2004; 13:2567-80.
52. Schirmer EC, Guan T, Gerace L. Involvement of the lamin rod domain in heterotypic lamin interactions important for nuclear organization. J Cell Biol 2001; 153:479-89.
53. Schirmer EC, Gerace L. The stability of the nuclear lamina polymer changes with the composition of lamin subtypes according to their individual binding strengths. J Biol Chem 2004; 279:42811-7.
54. Heitlinger E, Peter M, Lustig A, Villinger W, Nigg EA, Aebi U. The role of the head and tail domain in lamin structure and assembly: analysis of bacterially expressed chicken lamin A and truncated B2 lamins. J Struct Biol 1992; 108:74-91.
55. Stuurman N, Sasse B, Fisher PA. Intermediate filament protein polymerization: molecular analysis of Drosophila nuclear lamin head-to-tail binding. J Struct Biol 1996; 117:1-15.
56. Moir RD, Donaldson AD, Stewart M. Expression in *Escherichia coli* of human lamins A and C: influence of head and tail domains on assembly properties and paracrystal formation. J Cell Sci 1991; 99:363-72.
57. Schütz W, Benavente R, Alsheimer M. Dynamic properties of germ line-specific lamin B3: the role of the shortened rod domain. Eur J Cell Biol 2005; 84:649-62.
58. Von Moeller F, Barendziak T, Apte K, Goldberg MW, Stick R. Molecular characterization of Xenopus lamin LIV reveals differences in the lamin composition of sperms in amphibians and mammals. Nucleus 2010; 1:85-95.
59. Benavente R, Krohne G. Change of karyoskeleton during spermatogenesis of Xenopus: expression of lamin LIV, a nuclear lamina protein specific for the male germ line. Proc Natl Acad Sci USA 1985; 82:6176-80.
60. Clermont Y, Oko RHL. Cell biology of mammalian spermiogenesis. In: Desjardins C, Ewing LL, eds. Cell and molecular biology of the testis. New York, Oxford: Oxford University Press 1993; 332-76.
61. Kierszenbaum AL, Tres L. The acrosome-acroplaxome-manchette complex and the shaping of the spermatid head. Arch Histol Cytol 2004; 67:271-84.
62. Adelfalk C, Janschek J, Revenkova E, Blei C, Liebe B, Göb E, et al. Cohesin SMC1β protects telomeres in meiocytes. J Cell Biol 2009; 187:185-99.
63. Phair RD, Misteli T. High mobility of proteins in the mammalian cell nucleus. Nature 2000; 404:604-9.